Generalized Spectral Magnitude and Phase Retrieval Algorithm for Self-Referenced Multiheterodyne Detection

Anthony Klee, *Student Member, IEEE*, Josue Davila-Rodriguez, *Student Member, IEEE*, Charles Williams, *Student Member, IEEE*, and Peter J. Delfyett, *Fellow, IEEE*

***Abstract*—An algorithm for self-referenced spectral magnitude and phase retrieval of both optical frequency combs from a dual-comb multiheterodyne interferogram is rigorously defined. The algorithm is generalized to allow for the repetition rates of the two combs to be significantly different which allows for a reduction in required RF bandwidth. The validity of the algorithm is confirmed with an experimental demonstration.**

***Index Terms*—Frequency combs, multiheterodyne.**

I. Introduction

MULTIHETERODYNE or dual-comb detection has become a subject of interest recently due to its potential for rapid acquisition of high resolution and phase-sensitive spectral measurements. It has been utilized in a number of applications, including spectroscopy [1]–[4], length metrology [5]–[8], optical coherence tomography [9], and waveform measurement [10]–[13], which is of particular interest to this paper. Multiheterodyne detection is exceptionally well-suited for the measurement of waveforms that are difficult to characterize with now-conventional pulse measurement techniques like frequency resolved optical gating (FROG) and spectral phase interferometry for direct electric-field reconstruction (SPIDER) [14], [15]. High repetition rate pulse trains, which typically have lower peak power than that required for the nonlinear optical processes behind FROG and SPIDER, can be measured with relative ease as multiheterodyne detection is a low power, linear technique requiring just a photodetector and oscilloscope with sufficient bandwidth. Waveforms with large time-bandwidth products—for which well-defined and convergent FROG traces are prohibitively difficult to obtain—can also be characterized. These measurements are accomplished by effectively compressing and downconverting the complex optical comb spectra into the RF domain where the magnitude and phase of each combline can easily be characterized. In the downconverted spectrum though, the amplitude and phase information of the two optical combs are coupled, and so until recently it has been required that one of the optical frequency combs producing the multiheterodyne signal serve as a reference with either known complex spectrum so that its spectrum can be removed in post-processing or constant spectral magnitude and purely linear spectral phase such that the RF spectrum is an exact scaled version of the optical comb of interest [10], [11]. However, by utilizing higher frequency copies of the baseband spectrum, self-referenced measurements of the complex spectrum of each comb source can be simultaneously retrieved using a non-iterative algorithm, thus eliminating the requirement of a perfect reference comb [16], [17]. To minimize the RF bandwidth required for self-referenced retrieval, the repetition rate of one comb can be reduced to a small subharmonic of that of the comb of interest [17], though this increases the complexity of the retrieval algorithm. A form of this algorithm has previously been applied to the characterization of multiple semiconductor optical frequency comb sources [17], though only a cursory explanation of the algorithm was provided. In this paper, we present the mathematical basis for the generalized retrieval algorithm for both combs and experimentally verify its accuracy.

II. Magnitude and Phase Retrieval Algorithm

As described elsewhere and illustrated in Fig. 1, multiheterodyne detection of two optical frequency combs can produce a multitude of RF frequencies which group into distinct sets provided the carrier-envelope offset frequency and repetition rate of each comb are chosen carefully [11], [16], [17]. To obtain distinct sets with well-defined beat frequencies, the inequality expressed by (1) must be satisfied, in which N_B is the number of combines in the high repetition rate Comb B, Δ is the effective repetition rate difference, δ_o is the difference between the two nearest optical combines, and $f_{\mathrm{rep}}^{(A)}$ is the low repetition rate of Comb A.

$$(N_B - 1)\Delta + \delta_o < \frac{f_{\mathrm{rep}}^{(A)}}{2}. \tag{1}$$

Manuscript received May 23, 2013; revised September 1, 2013; accepted October 7, 2013. Date of publication October 17, 2013; date of current version November 11, 2013. This work was supported in part by the National Science Foundation under Contract DMR 0120967.

A. Klee and P. J. Delfyett are with CREOL, The College of Optics and Photonics, University of Central Florida, Orlando, FL 32816 USA (e-mail: acklee@creol.ucf.edu; delfyett@creol.ucf.edu).

J. Davila-Rodriguez was with CREOL, The College of Optics and Photonics, University of Central Florida, FL 32816 USA. He is now with Max Planck Institute of Quantum Optics, 85748 Garching, Germany (e-mail: jdavila@mpq.mpg.de).

C. Williams was with CREOL, The College of Optics and Photonics, at the University of Central Florida. He is now with FAZ Technology, Inc., Orlando FL 32826 USA (e-mail: charles.williams@faztechnology.com).

Color versions of one or more of the figures in this paper are available online at http://ieeexplore.ieee.org.

Digital Object Identifier 10.1109/JLT.2013.2286267

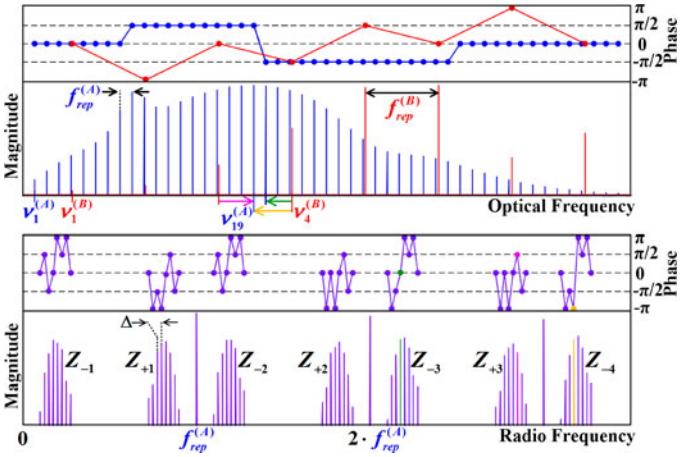

Fig. 1. (Color Online) Sample multiheterodyne optical spectrum (top) and RF spectrum (bottom). Comb A (Comb B) is shown in blue (red) with low (high) repetition rate $f_{\mathrm{rep}}^{(A)}$ ($f_{\mathrm{rep}}^{(B)}$). RF beats are spaced by the effective repetition rate difference, $\Delta = f_{\mathrm{rep}}^{(B)} - N_H \cdot f_{\mathrm{rep}}^{(A)}$, where N_H is the harmonic order or integer ratio of repetition rates ($\lfloor f_{\mathrm{rep}}^{(B)}/f_{\mathrm{rep}}^{(A)} \rfloor$) which is equal to 6 in this example. The number of comb lines in Comb B, N_B, is chosen to be 8 here.

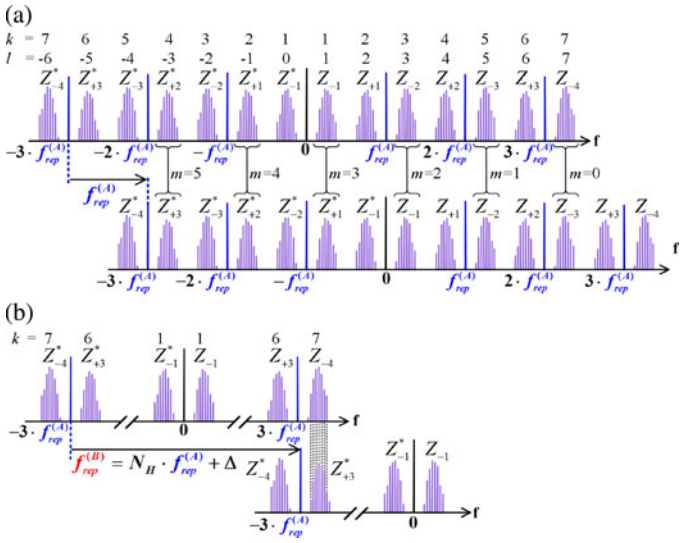

Fig. 2. Visual representation of retrieval algorithm for (a) low repetition rate comb and (b) high repetition rate comb. As in Fig. 1, $N_H = 6$ and $N_B = 8$.

With Δ limited to a minimum of the RF beat linewidth, (2) describes the maximum optical bandwidth that can be sampled without aliasing of beat frequencies occurring.

$$\mathrm{BW}_{\mathrm{opt}} = \frac{f_{\mathrm{rep}}^{(A)} \cdot f_{\mathrm{rep}}^{(B)}}{2\Delta}. \tag{2}$$

The heterodyne beat sets can be identified by their constituent optical comb lines. For optical spectra such as that shown in Fig. 1 where the frequency separation between Comb B and the nearest combline from Comb A increases with optical frequency, the lowest frequency beat set, Z_{-1}, consists of beats between each combline of Comb B and the closest lower frequency combline from Comb A. The second set, Z_{+1}, arises from Comb B beating with the closest higher frequency combline from Comb A. Subsequent sets continue this pattern, resulting from Comb B beating with the second closest lower and higher frequency lines from Comb A and so forth. As an example, consider the beat indicated with a green arrow between the $\nu_4^{(\mathrm{B})}$ combline in Comb B and the twentieth combline in Comb A. $\nu_{20}^{(\mathrm{A})}$ is the third closest lower frequency combline to the fourth combline in Comb B, and thus the beat between these two produces the RF tone $\mathrm{Z}_{-3}(4)$ shown in green, where $\mathrm{Z}_{-3}(4)$ refers to the complex amplitude of the fourth beat in the Z_{-3} set.

Being the product of comblines from each comb, the RF beat frequencies contain the spectral magnitude and phase information of both sources. The magnitude of $\mathrm{Z}_{-3}(4)$ is the product of the magnitudes of $\nu_{20}^{(\mathrm{A})}$ and $\nu_4^{(\mathrm{B})}$, $A_{20} \cdot B_4$, and the phase of $\mathrm{Z}_{-3}(4)$ is the optical phase difference, β_4-α_{20}. In order to isolate the spectrum of one comb, each beat must be referenced against a counterpart which contains information about a common optical combline [16], [17]. In doing so, the relationship between adjacent comblines within a single comb can be retrieved. Taking the ratio of $\mathrm{Z}_{-4}(4)$, the beat between $\nu_4^{(\mathrm{B})}$ and $\nu_{19}^{(\mathrm{A})}$ shown in orange in Fig. 1, to $\mathrm{Z}_{-3}(4)$ cancels the contribution of $\nu_4^{(\mathrm{B})}$ to yield the relationship between $\nu_{19}^{(\mathrm{A})}$ and $\nu_{20}^{(\mathrm{A})}$. Likewise, the ratio of $\mathrm{Z}_{-4}(4)$ to $\mathrm{Z}_{+3}^{*}(6)$, the conjugate of the beat between $\nu_3^{(\mathrm{B})}$ and $\nu_{19}^{(\mathrm{A})}$ shown in pink, cancels $\nu_{19}^{(\mathrm{A})}$ to yield the relationship between $\nu_3^{(\mathrm{B})}$ and $\nu_4^{(\mathrm{B})}$.

One method to determine which beats must be referenced against each other is to imagine two copies of the RF spectrum, one of which is shifted by the repetition rate of the comb to be retrieved, as shown in Fig. 2. Taking the ratio of beats that line up gives the magnitude and phase relationship between adjacent comblines in the comb of interest. In the optical domain, this is equivalent to referencing each adjacent combline pair within a comb to the line from the other comb nearest the midpoint of the pair. For example, when retrieving Comb A in Fig. 1, both the pair of $\nu_{15}^{(\mathrm{A})}$ and $\nu_{16}^{(\mathrm{A})}$ and the pair of $\nu_{18}^{(\mathrm{A})}$ and $\nu_{19}^{(\mathrm{A})}$ share $\nu_3^{(\mathrm{B})}$ as the common line to be cancelled, but the midpoint of $\nu_{19}^{(\mathrm{A})}$ and $\nu_{20}^{(\mathrm{A})}$ is closer to $\nu_4^{(\mathrm{B})}$ and so the reference point is changed. For Comb B, $\nu_{19}^{(\mathrm{A})}$ is the closest line to the midpoint of $\nu_3^{(\mathrm{B})}$ and $\nu_4^{(\mathrm{B})}$ and is thus used as the common point of reference. While any combline from the second comb can theoretically be chosen as the common reference for the retrieved pair, choosing the one closest to the pair's midpoint as done here represents the most efficient scheme, requiring the least amount of RF bandwidth.

To rigorously establish which beats to compare and in what order for retrieval of Comb A, first notice that if an index value is assigned to each RF beat set starting with $l = 1$ for the Z_{-1} set and continuing in each direction such that $l = 0$ for Z_{-1}^{*}, $l = 2$ for Z_{+1}, and so on, then the l_1 beat set in the original spectrum is always paired with the $l_2 = (l_1 - 2)$ set in the translated spectrum as seen in Fig. 2(a). Equation (3) gives the index values l_1 and l_2 for each of the two beat sets, where m is defined by (4) in terms of the optical combline index n of Comb A which runs from $n = 1$ to $n = N_H \cdot N_B - 1$ as shown in Fig. 1. The variable m effectively represents an index value for pairs of beat sets

starting with $m = 0$ for the most positive frequency pair and increasing to $m = N_H - 1$ for the most negative frequency pair. The last term in the expression for l_1 accounts for the parity of N_H, ensuring an incorrect mirror image of the spectrum is not recovered for odd values of N_H. From (3) it can be seen that retrieval requires knowledge of the first $N_H + 1$ beat sets, and so a minimum detection bandwidth of $(N_H + 1)\cdot f_{\mathrm{rep}}^{(A)}/2$ is necessary. This bandwidth approaches $f_{\mathrm{rep}}^{(B)}/2$ for large values of N_H [17].

$$l_1 = N_H + 1 - 2m - (N_H \bmod 2)\,; \quad l_2 = (l_1 - 2) \tag{3}$$

$$m = (n-1) \bmod N_H\,. \tag{4}$$

Computationally, it is more efficient to work with a single-sided RF spectrum, using half the amount of data in the double-sided spectrum, and so the beat set index l is converted to a single-sided spectrum beat set index k using (5), where *sgn* is the signum function.

$$k_{1,2} = \left| l_{1,2} + \frac{\mathrm{sgn}\,(l_{1,2}) - 1}{2} \right|. \tag{5}$$

While the transparency of the double-sided spectrum indexing is lost since $k_2 \neq (k_1 - 2)$ for negative values of l, retrieval can be performed more quickly by analyzing less spectrum and identifying fewer beat frequencies. The individual beat frequencies to be compared within the k_1 and k_2 beat sets are then given by their indices j_1 and j_2, respectively, in (6).

$$j_{1,2} = \mathrm{sgn}\,(l_{1,2}) \cdot \left[\left\lfloor \frac{n-1}{N_H} \right\rfloor + 1 - \frac{\mathrm{sgn}\,(l_{1,2}) - 1}{2} \times \left(N_B - 1 - 2\left\lfloor \frac{n-1}{N_H} \right\rfloor \right) \right]. \tag{6}$$

It should be noted that negative values of j indicate the complex conjugate of that beat is to be used. Finally, with $k_{1,2}$ and $j_{1,2}$, (7) can be applied to recover the magnitude ratio and phase difference of the n and $n + 1$ lines in Comb A.

$$\frac{A_n}{A_{n+1}} e^{i(\alpha_{n+1} - \alpha_n)} = \frac{Z_{(-1)^{k_1}\left\lfloor \frac{k_1+1}{2} \right\rfloor}(j_1)}{Z_{(-1)^{k_2}\left\lfloor \frac{k_2+1}{2} \right\rfloor}(j_2)}. \tag{7}$$

Having retrieved the relationships between adjacent comblines across the entire spectrum, one can easily calculate the magnitude and phase of all comblines relative to one reference combline arbitrarily chosen to have unity magnitude and zero phase. The choice of arbitrary initial combline magnitude translates to a scaling of the retrieved waveform average power, and the arbitrary choice of initial phase creates a constant phase offset across the entire spectrum, equivalent to a shift of the electric field relative to the retrieved waveform envelope in the time domain. For the purposes of this paper, we are not concerned with the field position, but only the shape of the intensity waveform.

The retrieval algorithm for Comb B illustrated in Fig. 2(b) is very similar in principle to that for Comb A, but can be greatly simplified as only two beat sets are required for the retrieval. Using the same beat set indexing schemes as before, the two beat sets of interest are identified by (8).

$$k_1 = N_H + 1 - (N_H \bmod 2)\,; \quad k_2 = N_H + (N_H \bmod 2)\,. \tag{8}$$

The RF combline index for the k_1 beat set is simply given by $j_1 = n + 1$, where n now is the optical combline index of Comb B running from $n = 1$ to $n = N_B$, and the RF combline index for the k_2 set is given by $j_2 = N_B + 1 - n$. Equation (9) then describes the proper ratio for recovery of the magnitude and phase relationship of adjacent comblines in Comb B. Note that the magnitude ratio in (9) is the reciprocal as compared to that in (7), and that the complex conjugate is always taken of the RF beat in the denominator.

$$\frac{B_{n+1}}{B_n} e^{i(\beta_{n+1} - \beta_n)} = \frac{Z_{(-1)^{k_1}\left\lfloor \frac{k_1+1}{2} \right\rfloor}(n+1)}{Z^*_{(-1)^{k_2}\left\lfloor \frac{k_2+1}{2} \right\rfloor}(N_B + 1 - n)}. \tag{9}$$

III. Post-Processing Considerations

While appropriate adjustment of mode spacing and offset frequency of each optical comb is imperative for producing an RF spectrum containing well-isolated and unaliased beat frequencies that are suitable for performing retrieval, proper acquisition and processing of the multiheterodyne signal is also vital. To obtain the complex RF spectrum, a fast Fourier transform (FFT) is calculated of the multiheterodyne signal which is digitized by a high speed, real-time oscilloscope. In calculating the FFT, it is desired that the heterodyne beats fall exactly on the points or bins in the FFT vector so as to avoid scalloping losses and to get an accurate measure of the beats' magnitude and phase. Towards this end, the duration of the signal to be transformed is chosen to be an integer multiple of the period corresponding to the effective repetition rate difference of the two comb sources. That is to say, $T_s = a\cdot T_p = b/\Delta$ where T_s is the duration of the signal, T_p is the oscilloscope sampling period, Δ is the effective repetition rate difference, and a and b are integers. Doing so maps the separation between beat frequencies to an integer number of FFT points such that the same segment of the (implicit or explicit) time-domain windowing function's frequency response is consistently sampled.

This exact mapping is not always possible however, as the sampling period of the oscilloscope may not be commensurate with the signal period ($1/\Delta$), in which no integers a and b exist that satisfy $a\cdot T_p = b/\Delta$. In other cases, a and b may exist, but only if T_s is allowed to become very long, at which point one must consider the upper limit on acquisition time imposed by the coherence time of the two comb sources. If the comb sources are phase locked to a common stable reference, it is possible to acquire coherent signals over long times ($\sim$1 s) and achieve correspondingly high frequency resolution in the Fourier spectrum [2]. In the results shown in this paper, the maximum acquisition time was limited to $\sim$10 μs by the $\sim$100 kHz optical linewidth of the low repetition rate comb. With this time constraint, the constant sampling rate of 25 GS/s dictated by the DAQ card of the oscilloscope, and Δ set by the comb repetition rates, we were unable to identify values of a and b satisfying the above relationship, resulting in a small slippage

between beat peaks and FFT bins. As the retrieval algorithm is based on taking the complex ratio of beats which now have different amounts of scalloping loss, this slippage introduces compounding error which ends up dramatically distorting the retrieved spectrum. As a note, scalloping losses were found to affect the retrieved magnitude more severely than the retrieved phase due to scalloping losses in phase being linear with shallow slope while losses in magnitude are nonlinear and increase much more rapidly.

To rectify these errors, several options exist, the simplest of which is to choose a smoother time-domain windowing function than the implicit rectangular window to apply to the signal before transforming. A Hann window has been applied to all data shown here to reduce the maximum scalloping loss as well as diminish the effect of sidelobes on neighboring beats by providing superior sidelobe suppression as compared to a rectangular window. The classic approach to mitigating scalloping loss by using a flattop window is unsuitable for this application due to its poor frequency resolution obfuscating the center location of each beat frequency. While windowing helps to improve retrieved magnitude accuracy, the error due to beats not being separated by an integer number of FFT bins must still be corrected. A beat's true magnitude may be estimated by increasing the frequency resolution through transformation of longer duration signals, but again the issue of signal coherence time is encountered. Alternatively, the length of windowed signal can be held constant while zero-padding to achieve arbitrarily fine interpolation of the frequency spectrum, but this becomes too computationally intensive for long lengths. It is also possible to concentrate the power in each beat to a single bin by performing phase error correction. This can be accomplished by multiplying the original multiheterodyne signal by the inverse of the temporal phase fluctuations of individually filtered beat tones.

The approach taken here was to hold the length of windowed signal constant (i.e. fixed frequency resolution) but incrementally zero-pad the vector to compute multiple FFTs of marginally different lengths, effectively sweeping the FFT points across the multiheterodyne spectrum. The frequency, magnitude, and phase of all relevant beats were tracked for 22 FFTs of different lengths and aggregated to provide a more accurate picture of the RF spectrum with improved sampling density. The results of this process are shown in Fig. 3 along with a sample FFT. As one can see, a single FFT fails to accurately capture the true magnitude of all beats simultaneously. Even between two adjacent beats, as displayed in the inset, there is significant slippage of the FFT bins relative to the beat peaks due to a non-integer number of signal periods being transformed. By fitting the beat peaks to the frequency response of the windowing function, an accurate measure of the beat's magnitude and center frequency can be obtained. The center frequency is then used in a linear fit of the phase values to calculate the beat's true phase.

In addition to the accurate magnitude and phase measurements, one benefit of this multiple aggregated FFTs approach is the improved processing time. Using 22 different short FFTs ($\sim 10^5$ samples) is an order of magnitude faster than a single long FFT ($\sim 10^7$ samples) that achieves the same effective point

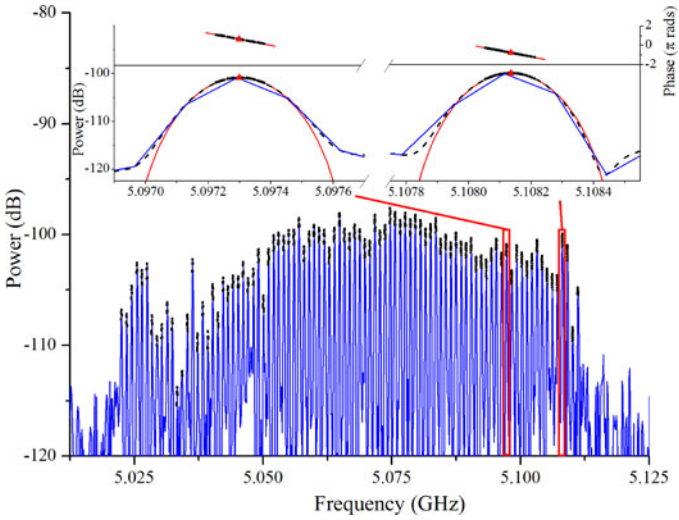

Fig. 3. (Color Online) Sample heterodyne beat set from multiheterodyne spectrum. A single FFT is shown in blue and the peak locations from 22 FFTs are shown as black dots. Inset: Detail of two adjacent beats. Fits to magnitude and phase plotted in red, with beat center indicated by the red triangle. Dashed black lines indicate interpolated lineshapes via a single FFT zero-padded by a factor of 100.

density seen in Fig. 3 inset. If the low repetition rate reference comb is disregarded and only the signal comb retrieved, the total computation time is less than 10 seconds. In contrast, using a single long FFT to perform retrieval takes several minutes. With processing time of seconds, this algorithm enables high accuracy, near real-time complex spectral measurements.

IV. Experimental Demonstration

To verify the correctness of the retrieval algorithm and demonstrate the applicability of the measurement technique to high repetition rate, arbitrarily shaped pulse trains, we attempted to measure the spectral phase of a widely spaced frequency comb after applying a known phase mask using a commercial spectral processor based on a liquid crystal on silicon spatial light modulator (SLM). The frequency comb to be shaped (Comb B) was produced by a harmonically mode-locked semiconductor laser with a tunable repetition rate around 10.25 GHz [18]. The second frequency comb (Comb A) against which to beat Comb B was a commercially available, carrier-envelope offset stabilized, mode-locked fiber laser with 250 MHz repetition rate. For the purposes of this experiment the repetition rate of Comb B was tuned to 10.251 GHz to give $N_H = 41$ and $\Delta \approx 1$ MHz, thus requiring an RF bandwidth of just 5.25 GHz as opposed to 10.251 GHz if measured with a second $\sim$10.25 GHz comb ($N_H = 1$) [17]. The experimental setup to record the interferogram between the two combs consisted of passing Comb B through the spectral processor while Comb A was stretched in a chirped fiber Bragg grating (CFBG) to reduce the peak pulse power and improve the dynamic range. A polarization controller was used after the CFBG to best match polarizations and then the combs were mixed and photodetected.

With the spectral processor in the system but prior to applying any amplitude or phase mask, a baseline interferogram

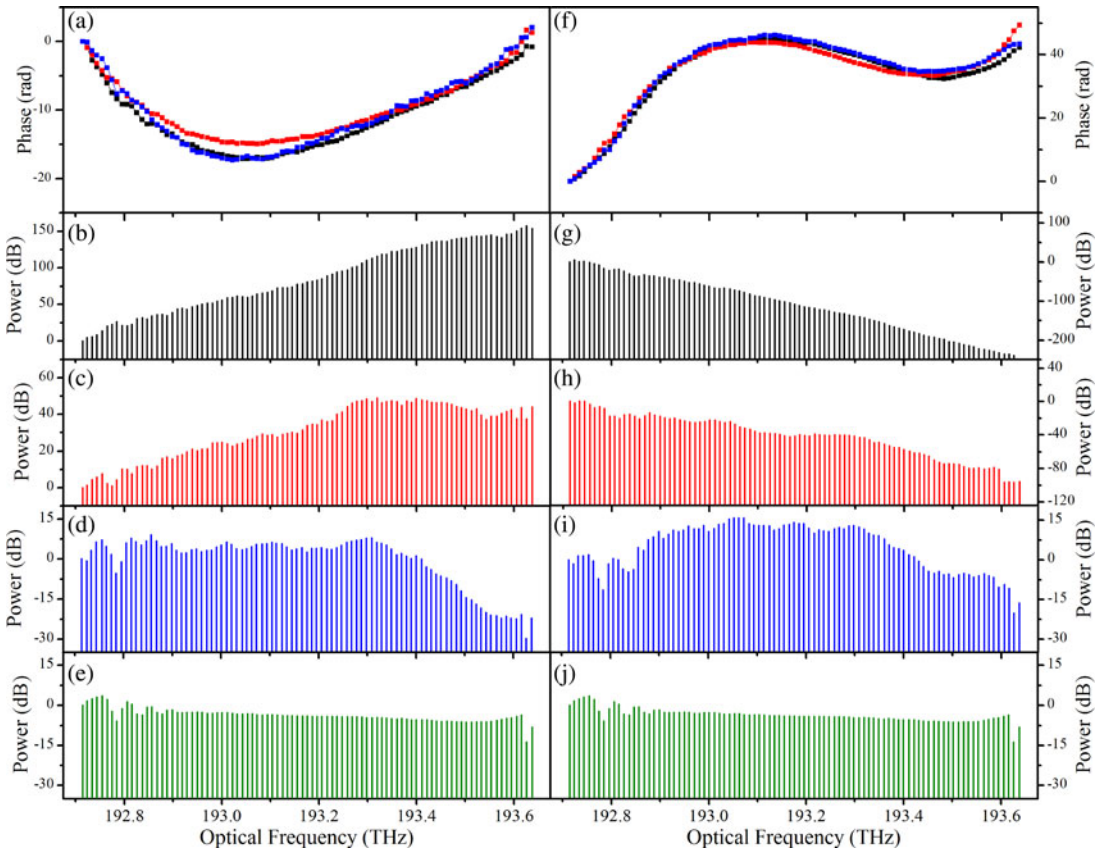

Fig. 4. (Color Online) Retrieved spectral phase (a) and (f) and magnitude (b)–(d), (g)–(i) of high repetition rate comb with comparison of different postprocessing methods. The spectrum as measured on an optical spectrum analyzer is shown in (e) and (j) for reference. The left column of data was taken with no phase mask applied to the spectral processor, while a positive cubic phase mask was applied for the data on the right. Second row (in black) indicates retrieved spectra with rectangular window. Third row (in red) indicates retrieved spectra with Hann window. Fourth row (in blue) indicates retrieved spectra with Hann window and multiple aggregated FFTs. Note the independent vertical scales for each plot, though (d), (e), (i), (j) are plotted on same scale.

was recorded and the spectrum shown on the left in Fig. 4 was retrieved for Comb B. To show the improvement in retrieval accuracy of our algorithm, we have processed the data three different ways: 1) Using a single FFT with a simplistic rectangular windowing function, shown in black, 2) Using a single FFT with a Hann windowing function, shown in red, and 3) Using multiple FFTs as presented in Section III with a Hann window, shown in blue. The retrieved phase for each of these cases is plotted in Fig. 4(a), exhibiting consistent behavior despite the different processing methods. Fitting the blue phase profile to the third order Taylor polynomial of (10) yielded a quadratic phase coefficient of $\Phi_2 = 4.21$ ps^2 and a cubic phase coefficient of $\Phi_3 = -2.05$ ps^3.

$$\Phi = \Phi_0 + \Phi_1 (\omega - \omega_o) + \frac{\Phi_2}{2!}(\omega - \omega_o)^2 + \frac{\Phi_3}{3!}(\omega - \omega_o)^3 . \tag{10}$$

In contrast to the phase, the retrieved magnitude varies greatly depending on processing method, with largely different shapes and ranges of power. This can be explained by considering the frequency response of the windowing functions. As seen in Fig. 3 inset, if the frequency response is sampled at some offset from peak center, the phase is shifted by some small linear amount while the magnitude rapidly drops nonlinearly. Comparing to the spectrum measured on an optical spectrum analyzer and shown in Fig. 4(e), using a rectangular window causes enormous distortion of the spectrum with a range in excess of 150 dB. Using a Hann window helps to flatten the spectrum, but still produces significant distortion and erroneously predicts increasing power with optical frequency. Aggregating multiple FFTs to predict the true magnitude and phase of RF beats offers clear improvement, with the retrieved spectrum exhibiting the same scale, similar flatness, and distinct features as the measured reference. There is a drop in power at high frequency though, resulting from errors in the calculated magnitude ratio of the beats from those comblines.

These errors are thought to be due to two factors in this experiment. First, even with adjustment of the polarization controller, Comb A was observed to lack a uniform state of polarization after the CFBG, causing distortions in the photodetected power spectrum as not all comblines were co-polarized with Comb B. This effect would directly create errors in the retrieved magnitude though not the retrieved phase. In future work, inclusion of a polarizing element after the CFBG to force a uniform state of polarization is expected to mitigate this error. Secondly, the relatively broad optical linewidth of Comb A ($\sim$100 kHz) introduces noise in both the magnitude and phase of the RF beats when beating with Comb B. A comb with narrower linewidth

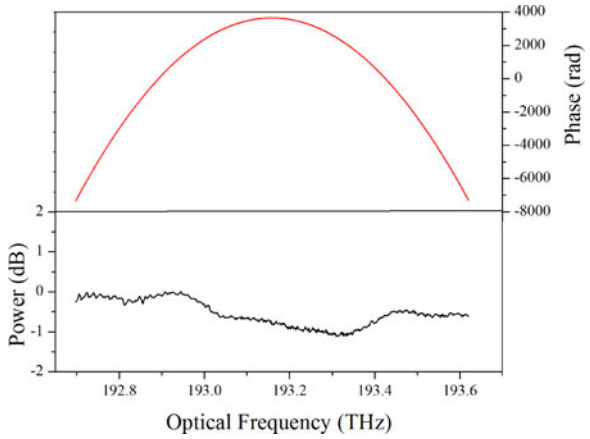

Fig. 5. Retrieved spectral phase and measured spectral magnitude of 250 MHz frequency comb (Comb A). The spectral phase is primarily shaped by the dispersion of the CFBG.

will reduce this source of error as well as increase the maximum acquisition time, and magnitude retrieval should be possible. Ultimately however, this issue is not of great concern since the retrieved spectral intensity can be discarded in favor of the easily measured spectrum, similar to what is done in other spectral phase measurement techniques such as FROG.

The spectral processor was then used to apply a purely cubic phase mask with $\Phi_3 = 12.09\ \text{ps}^3$ to the output of Comb B. A second interferogram was recorded with the phase mask applied, yielding the spectra in the right column of Fig. 4 upon retrieval. The retrieved phase in Fig. 4(f) is again consistent regardless of processing method, with fit coefficients of $\Phi_2 = 4.21\ \text{ps}^2$ and $\Phi_3 = 10.05\ \text{ps}^3$ for the blue profile. Comparing these coefficients to those obtained without the phase mask applied, the second-order phase coefficient remained constant, as expected in absence of any quadratic phase change from the mask. The change in the third-order phase coefficient of $\Delta\Phi_3 = 12.10\ \text{ps}^3$ is in excellent agreement with the applied mask's cubic coefficient with less than 0.1% error. Similar to the first data set, the retrieved magnitude is observed to be extremely distorted with a rectangular window (4g) and marginally improved with a Hann window (4h). The third approach again produces a flattened spectrum (4i), comparable to the measured spectrum (4j) with the same range.

Using the same interferogram, the spectral phase of Comb A was also retrieved and can be seen in Fig. 5. Though all fiber and optical components between the comb source itself and the photodetector contribute to shaping the spectral phase, it is expected to be predominantly determined by the highly dispersive CFBG which has a specified dispersion of 2044.64 ps/nm at 1554 nm. The retrieved phase profile is fit with a quadratic phase coefficient of $\Phi_2 = -2616.21\ \text{ps}^2$, equivalent to dispersion of 2042.43 ps/nm at 1554 nm which is just 0.1% less than the specification.

V. Conclusion

We have presented a generalized algorithm for self-referenced spectral retrieval from a dual-comb interferogram. By referencing particular beat frequencies against each other, independent measurements of the magnitude and phase of both optical frequency combs can be obtained, removing constraints on the spectral flatness of the reference comb. The generalized algorithm facilitates a reduction of the repetition rate of one comb source to a small subharmonic of that of the second comb, which reduces the RF bandwidth required to perform retrieval.

We experimentally tested the algorithm by applying a known phase mask to one comb and extreme linear dispersion to the other. For both combs, the retrieved phase exhibited less than 0.1% difference from the expected values, demonstrating superb phase accuracy. By aggregating multiple FFTs of different lengths, we have significantly improved the retrieved magnitude. In summary, this algorithm represents a rapid, efficient, and accurate technique for the measurement and characterization of low power, high repetition rate, or large time-bandwidth product waveforms.

References

[1] A. Schliesser, M. Brehm, F. Keilmann, and D. W. van der Weide, "Frequency-comb infrared spectrometer for rapid, remote chemical sensing," *Opt. Exp.*, vol. 13, no. 22, pp. 9029–9038, Oct. 31, 2005.

[2] I. Coddington, W. C. Swann, and N. R. Newbury, "Coherent multiheterodyne spectroscopy using stabilized optical frequency combs," *Phys. Rev. Lett.*, vol. 100, no. 1, p. 013902, Jan. 2008.

[3] B. Bernhardt, A. Ozawa, P. Jacquet, M. Jacquey, Y. Kobayashi, T. Udem, R. Holzwarth, G. Guelachvili, T. W. Hansch, and N. Picque, "Cavity-enhanced dual-comb spectroscopy," *Nat. Photon.*, vol. 4, no. 1, pp. 55–57, Jan. 10, 2010.

[4] E. Baumann, F. R. Giorgetta, W. C. Swann, A. M. Zolot, I. Coddington, and N. R. Newbury, "Spectroscopy of the methane nu(3) band with an accurate midinfrared coherent dual-comb spectrometer," *Phys. Rev. A*, vol. 84, no. 6, p. 062513, Dec. 28, 2011.

[5] I. Coddington, W. C. Swann, L. Nenadovic, and N. R. Newbury, "Rapid and precise absolute distance measurements at long range," *Nat. Photon.*, vol. 3, no. 6, pp. 351–356, Jun. 2009.

[6] M. Bagnell, J. Davila-Rodriguez, C. Williams, and P. J. Delfyett, "Multiheterodyne detection and sampling of periodically filtered white light for correlations at 20 km of delay," *IEEE Photon. J.*, vol. 4, no. 2, pp. 504–511, Apr. 2012.

[7] T. A. Liu, N. R. Newbury, and I. Coddington, "Sub-micron absolute distance measurements in sub-millisecond times with dual free-running femtosecond Er fiber-lasers," *Opt. Exp.*, vol. 19, no. 19, pp. 18501–18509, Sep. 12, 2011.

[8] M. Godbout, J. D. Deschenes, and J. Genest, "Spectrally resolved laser ranging with frequency combs," *Opt. Exp.*, vol. 18, no. 15, pp. 15981–15989, Jul. 19 2010.

[9] S. Kray, F. Spöler, M. Först, and H. Kurz, "Dual femtosecond laser multiheterodyne optical coherence tomography," *Opt. Lett.*, vol. 33, no. 18, pp. 2092–2094, 2008.

[10] F. Ferdous, D. E. Leaird, C. B. Huang, and A. M. Weiner, "Dual-comb electric-field cross-correlation technique for optical arbitrary waveform characterization," *Opt. Lett.*, vol. 34, no. 24, pp. 3875–3877, Dec. 2009.

[11] J. Davila-Rodriguez, M. Bagnell, C. Williams, and P. J. Delfyett, "Multiheterodyne detection for spectral compression and downconversion of arbitrary periodic optical signals," *J. Lightw. Technol.*, vol. 29, no. 20, pp. 3091–3098, Oct. 2011.

[12] I. Coddington, F. R. Giorgetta, E. Baumann, W. C. Swann, and N. R. Newbury, "Characterizing fast arbitrary CW waveforms with 1500 THz/s instantaneous chirps," *IEEE J. Sel. Topics Quantum Electron.*, vol. 18, no. 1, pp. 228–238, Jan./Feb. 2012.

[13] F. R. Giorgetta, I. Coddington, E. Baumann, W. C. Swann, and N. R. Newbury, "Fast high-resolution spectroscopy of dynamic continuous-wave laser sources," *Nat. Photon.*, vol. 4, no. 12, pp. 853–857, Dec. 2010.

[14] C. Iaconis and I. A. Walmsley, "Spectral phase interferometry for direct electric-field reconstruction of ultrashort optical pulses," *Opt. Lett.*, vol. 23, no. 10, pp. 792–794, May 1998.

[15] R. Trebino, *Frequency-Resolved Optical Gating: The Measurement of Ultrashort Laser Pulses*. New York, NY, USA: Springer, 2000.
[16] N. K. Fontaine, D. J. Geisler, R. P. Scott, and S. J. B. Yoo, "Simultaneous and self-referenced amplitude and phase measurement of two frequency combs using multi-heterodyne spectroscopy," in *Proc. Opt. Fiber Commun. Conf.*, Mar. 2012, pp. 1–3, Paper OW1 C.1.
[17] A. Klee, J. Davila-Rodriguez, C. Williams, and P. J. Delfyett, "Characterization of semiconductor-based optical frequency comb sources using generalized multiheterodyne detection," *IEEE J. Sel. Topics in Quantum Electron.*, vol. 19, no. 4, pp. 1100711–1100711, 2013.
[18] C. Williams, J. Davila-Rodriguez, K. Bagnell, and P. J. Delfyett, "Stabilization of an injection locked harmonically mode-locked laser via polarization spectroscopy for frequency comb generation," in *Proc. Lasers Electro-Opt. Conf. Quantum Electron. Laser Sci.*, May 2012, pp. 1–2, Paper JTH2 A.50.

Anthony Klee (S'11) received the B.S. degree in optical engineering from Rose–Hulman Institute of Technology in 2010, the M.S. degree in optics from the University of Central Florida in 2013, and is currently working toward the Ph.D. degree in optics from the Center for Research and Education in Optics and Lasers (CREOL) at UCF.

He is a Graduate Research Assistant at CREOL in Orlando, FL, USA. His research interests include the generation of optical frequency combs from semiconductor mode-locked lasers and the development of novel measurement techniques for the characterization of these combs.

Mr. Klee is a student member of IEEE Photonics Society.

Josue Davila-Rodriguez (S'11) received the B.S. degree in engineering physics from Tecnologico de Monterrey in 2006 and joined the Center for Research and Education in Optics and Lasers, the University of Central Florida in 2007. He received the Ph.D. degree in optics from the University of Central Florida in 2013.

He is currently a Research Scientist at the Max Planck Institute of Quantum Optics in Garching, Germany. His research interests include novel mode-locked laser sources and applications.

Charles Williams (S'06) received the B.S. degree in physics from the University of Missouri – Rolla in 2006, the M.S. degree in optics from the University of Central Florida in 2008, and the Ph.D. degree in optics in 2013, also from the University of Central Florida.

He is currently a senior member of the technical staff at FAZTechnology, Inc. in Orlando, FL, USA. His research interests include the creation of low-noise oscillators and optical comb sources for communications, laser ranging, and signal processing—namely through the use of injection locking techniques. Dr. Williams is a member of IEEE Photonics Society.

Peter J. Delfyett (S'79–M'94–SM'96–F'02) received the Ph.D. degree in electrical engineering from the City University of New York, New York, NY, USA, in 1988. He is the University of Central Florida Trustee Chair Professor of Optics, EE and Physics, The College of Optics and Photonics, and the Center for Research and Education in Optics and Lasers (CREOL), University of Central Florida. Prior to this, he was a member of the Technical Staff at Bell Communications Research from 1988–1993.

Dr. Delfyett served as the Editor-in-Chief of the IEEE JOURNAL OF SELECTED TOPICS IN QUANTUM ELECTRONICS (2001–2006), and served on the Board of Directors of the Optical Society of America. He served as an Associate Editor of IEEE PHOTONICS TECHNOLOGY LETTERS, and was the Executive Editor of IEEE LEOS NEWSLETTER (1995–2000). He is a Fellow of the Optical Society of America, Fellow of IEEE Photonics Society, and Fellow of the American Physical Society. He was also a member of the Board of Governors of IEEE-LEOS (2000–2002) and a member of the Board of Directors of the Optical Society of America (2004–2008). In addition, Dr. Delfyett has been awarded the National Science Foundation's Presidential Faculty Fellow Early Career Award for Scientists and Engineers, which is awarded to the Nation's top 20 young scientists. He has published more than 650 articles in refereed journals and conference proceedings, has been awarded 35 United States Patents. He was awarded the University of Central Florida's 2001 Pegasus Professor Award which is the highest honor awarded by the University. Dr. Delfyett has also endeavored to transfer technology to the private sector, and helped to found "Raydiance, Inc." which is a spin-off company developing high power, ultrafast laser systems, based on Dr. Delfyett's research, for applications in medicine, defense, material processing, biotech, and other key technological markets. Most recently, he was awarded the APS Edward Bouchet Award for his significant scientific contributions in the area of ultrafast optical device physics and semiconductor diode based ultrafast lasers, and for his exemplary and continuing efforts in the career development of underrepresented minorities in science and engineering.